Title	Simultaneous measurement of gamma-ray energy spectrum and dose in real-time up to 3 MeV with CsI(Tl) scintillator-based prototype monitor
Author(s)	Voulgaris, Nikolaos; Qiu, Jiye; Tamaki, Shingo et al.
Citation	Radiation Measurements. 2026, 194, p. 107683
Version Type	VoR
URL	https://hdl.handle.net/11094/104847
rights	This article is licensed under a Creative Commons Attribution 4.0 International License.
Note	

Radiation Measurements 194 (2026) 107683

Contents lists available at ScienceDirect

Radiation Measurements

journal homepage: www.elsevier.com/locate/radmeas

Simultaneous measurement of gamma-ray energy spectrum and dose in real-time up to 3 MeV with CsI(Tl) scintillator-based prototype monitor

Nikolaos Voulgaris *, Jiye Qiu, Shingo Tamaki, Sachie Kusaka, Isao Murata

Division of Sustainable Energy and Environmental Engineering, Graduate School of Engineering, The University of Osaka, Yamadaoka 2-1, Suita, Osaka, 565-0871, Japan

ARTICLE INFO

Keywords:
Gamma-ray spectroscopy
Real-time radiation monitoring
Spectrum unfolding
CsI(Tl) scintillator
MPPC
Dose rate

ABSTRACT

In medical applications of radiation, the priority is always the exposure and dosimetry of the patient. However, medical workers are also frequently exposed to radiation. A variety of dosimeters are used by medical workers, but they often have limitations. For this purpose, we are developing a lightweight monitor that can measure the energy spectrum and dose rate of gamma-rays simultaneously and accurately in real-time. The monitor mainly consists of a CsI(Tl) scintillator coupled to an MPPC. To obtain the unfolded energy spectrum, we utilize an improved sequential Bayesian estimation. This study experimentally confirms that the prototype monitor can identify gamma-rays up to around 3 MeV, a common upper limit in medical environments using radiation. To achieve this, we measured the 2.755 MeV gamma-rays emitted from ^{24}Na. As a result, the gamma-ray energy peaks were displayed in real-time, and the dose rate was measured quickly and accurately.

1. Introduction

The use of radiation in medicine has increased dramatically in recent years, encompassing therapies like gamma knife and brachytherapy as well as those that utilize accelerators such as medical linear accelerator (LINAC), proton, heavy-ion and boron neutron capture therapy (Donadille et al., 2008; Sasaki and Fujibuchi, 2020; Matsumura et al., 2022). Diagnostics such as positron emission tomography (PET), computed tomography (CT) and radiopharmaceuticals comprise another major part of the medical applications of radiation (Sasaki and Fujibuchi, 2020). To minimize exposure, apart from shielding and proper staff training, precise and real-time monitoring is necessary to ensure safety for patients and staff alike (IAEA, 2018). Consequently, various dosimeters and monitors are employed in radiation monitoring (MoE, 2019). Current devices like electronic personal dosimeters (EPDs), have advanced significantly in size reduction and enhanced functionality such as dose rate alarms, yet can still face challenges such as accuracy and susceptibility to electromagnetic interference (Ortega and Ginjaume, 2000). Additionally, integrating personal dosimeters like optically stimulated luminescence (OSL), thermally stimulated luminescence (TSL), and radiophotoluminescence (RPL) dosimeters provide the total dose exposure over a set period, typically 1-3 months, providing no real-time information (Lakhwani et al., 2019; Yamamoto et al., 2020; Yanagida et al., 2022). There are also instances of inconsistent adherence to dosimeter usage among healthcare staff, despite institutional efforts to promote safety (Qureshi et al., 2022; Lee et al., 2022; Piotrowski et al., 2021). Furthermore, many dosimeters and survey meters are calibrated using a single standard gamma-ray source, like ^{137}Cs which emits 0.662 MeV gamma-rays. These devices can exhibit poor response at energies higher or lower than this calibration point (Meier and Kappadath, 2015), leading to underestimation or overestimation of the dose rate, respectively (Nishimura et al., 2022). Devices capable of displaying the pulse height spectrum of gamma-rays, as well as the dose rate, typically weigh over 1 kg, as is the case with the RayMon10 (Kromek, Durham, UK) and Radeaglet-R (ORTEC, Oak Ridge, USA). Those that only display the dose rate are much lighter, such as the DMC 3000, RDS 30 (Mirion Technologies, Atlanta, USA, 2023 and 2022 respectively) and DKG-09D (Buzhan et al., 2018) (SPC Doza, Moscow, Russia, 2017), weighing around 90-300 g but can exhibit high deviation at energies far from 0.662 MeV (^{137}Cs).

In this paper, we highlight the latest advancements made by our research group in developing a portable gamma-ray monitor that strives to provide an answer to the above issues. In response to the growing need for effective radiation monitoring, the monitor used in this study

This article is part of a special issue entitled: Scintillators Applications published in Radiation Measurements.

* Corresponding author.
E-mail addresses: voulgaris.nikolaos@qr.see.eng.osaka-u.ac.jp (N. Voulgaris), murata@see.eng.osaka-u.ac.jp (I. Murata).

https://doi.org/10.1016/j.radmeas.2026.107683
Received 9 November 2025; Received in revised form 2 March 2026; Accepted 22 March 2026
Available online 23 March 2026

can measure the energy spectrum and dose of gamma-rays simultaneously in real-time, combining the portability of a dosimeter and the detailed information of a spectrometer, with the added benefit of displaying the true gamma-ray energy spectrum, not just the pulse height distribution. The unfolded energy spectrum contains the true information of the incoming gamma-rays (Sarzi Amadè et al., 2020), which aids in easy radionuclide identification and mainly serves as a means to calculate in real-time the dose rate, by applying a flux-to-dose conversion coefficient to the unfolded energy spectrum (ICRP, 1997; Otto, 2016). Unlike the methods of some devices described above that are calibrated with a specific nuclide like ^{137}Cs, our method can provide accurate readings at energies further away from this value as well because the flux-to-dose conversion coefficient increases monotonically with the increase of gamma-ray energy.

The primary objective of this research is to cater to medical radiation workers and enhance their understanding and awareness of radiation exposure. For this purpose the monitor is designed to be lightweight and wearable, with the final size and weight estimated to be similar to a modern smartphone (~250 g).

To realize the commercial potential of the monitor, we have confirmed in studies conducted so far that the sequential Bayesian estimation method can be used to measure the energy spectrum and dose rate, thus verifying the feasibility of the methodology (Kobayashi et al., 2017). The improved sequential Bayesian estimation, named *k*-α method, has been compared with results obtained from the standard sequential Bayesian estimation (α method) and evaluated with standard gamma-ray sources (~6 μSv/h dose rates) (Murata et al., 2024). Additionally, the accuracy of the dose rate estimation has been confirmed in various conditions. These include experiments in background (0.08 μSv/h), with standard gamma-ray sources (^{133}Ba, ^{137}Cs, ^{22}Na, ^{60}Co) (Nishimura et al., 2022; Voulgaris et al., 2023) and in front of a nuclear fuel storage room (2 μSv/h). The latter consisting of UO_2 pellets that were used as critical assembly fuel and after 50 years emit complex gamma-ray spectra, similar to that in a typical medical radiation field. In summary, using the sequential Bayesian estimation method, unfolding of the gamma-ray spectra and estimation of the dose rate can be successfully performed not only in simple environments like the background or monoenergetic gamma-ray sources, but also in a more complex environment where many gamma-rays are present (Nishimura et al., 2022). However, the tested upper gamma-ray energy so far was 1.3 MeV, which does cover most gamma-ray emitting nuclides used as radiopharmaceuticals (Alsaab and Zeghib, 2023; Nuclear Regulation Authority, 2017), but not some high energy emitting nuclides like ^{124}I (1.691 MeV) (Bakshi and Chu, 2020). It also does not cover the full range of energies present in facilities that utilize accelerators (Sharma and Sarkar, 2020; Polaczek-Grelik et al., 2019).

This research aims to expand on our efforts so far and verify that the prototype monitor can accurately display the unfolded energy spectrum and the dose rate of gamma-rays with energies of up to around 3 MeV. In the context of medical environments using particle accelerators, the gamma-ray spectrum extends mainly up to about 3 MeV, as this range includes most of the gamma-rays produced after operation, such as due to the activation of accelerator components, and includes LINAC, accelerator based neutron capture therapy, proton therapy, heavy ion therapy and others (Polaczek-Grelik et al., 2019; Długosz-Lisiecka et al., 2023; Matsumura et al., 2022). Additionally, the normalization of measurement ranges to a maximum of around 3 MeV, aligning with standard practices in radiation monitoring (Moiseev and Lukina, 2020), emphasizing the need for measuring instruments to cover this range to ensure accuracy and reliability in various operational settings, like medical facilities. Consequently, this value has been selected as the peak energy range for various commercial dose rate meters, such as the RDS-30 (Mirion Technologies, Atlanta, GA, USA, 2022), minitrace-γ (Bertin Technologies, Paris, France, 2023), RadEye PRD series (Thermo-Fischer Scientific, Waltham, Massachusetts, USA) for high dose rates and DKG-09D (Buzhan et al., 2018) (SPC Doza, Moscow, Russia, 2017) among others.

Since there are no available standard gamma-ray sources with such high energies, we utilize the reaction of ^{27}Al(n,α)^{24}Na to produce gamma-rays of energies 1368.6 keV and 2754.6 keV (Nakao et al., 2021). The dose rate is measured with the prototype monitor, an NaI survey meter and additionally, the theoretical dose rate value was calculated. They are compared with each other to finally confirm the effectiveness of the present monitor. As stated in prior publications in the development of this monitor (Murata et al., 2024), the intended dose range is approximately 0.05 μSv/h (background levels) up to 1 mSv/h, corresponding to typical radiation levels encountered in medical and controlled-area environments. A future goal is to extend this to 10 mSv/h.

2. Materials and methods

2.1. Materials

The prototype monitor primarily consists of a CsI(Tl) scintillator (2.6 × 2.6 × 2.6 cm^3, provided by I.S.C.Lab. CO.,LTD, Osaka, Japan), a multi-pixel photon counter (MPPC, C14047-0436, Hamamatsu photonics, Hamamatsu, Japan), an amplifier (ORTEC575A, ORTEC/AMETEK, Oak Ridge, USA, shaping time 3 μs) and the DP5, a digital pulse processor and multi-channel analyzer (Amptek Inc, Bedford, MA, USA) (AMPTEK). MPPCs have been widely coupled with various scintillators (Kato et al., 2013; Okazaki et al., 2023), including CsI(Tl) (Torigoe et al., 2019; Jasni et al., 2021), and have advantages in terms of their small size, being lightweight and having high signal amplification gain and insensitivity to magnetic interference (Kato et al., 2013; Kataoka et al., 2015). They have high quantum efficiency and mechanical robustness, and are an energy-efficient alternative to traditional photomultiplier tubes (PMTs) with sensitivity across a wide wavelength range (Ghassemi et al., 2022). Regarding the selection of scintillator material, CsI(Tl) is known to be compatible with MPPC in terms of maximum emission wavelength, it is only slightly hygroscopic and has an affordable price (Jasni et al., 2021; Knoll, 2010). It is an established material and multiple studies have confirmed its applicability in radiation detection systems (Risse et al., 2023; Pereira et al., 2015; Yanagida, 2018). It has also been applied successfully to various portable hand-held gamma-ray detector systems (Buzhan et al., 2018; Risse et al., 2023). Dead time was an important consideration of the initial system design. The use of the DP5 digital pulse processor reduces processing dead time and pulse pile-up. The design criteria of the initial system design are expanded in further detail in prior work introduced in section 1, covering feasibility investigations (Kobayashi et al., 2017), experimental investigations (Nishimura et al., 2022) and break down of the developed estimation method (Murata et al., 2024).

A diagram of the setup is presented in Fig. 1, where the main components can be identified.

Fig. 2 is a photograph of the main components of the prototype monitor, where the CsI(Tl) scintillator is wrapped in tape and lastly with aluminum. Specifically, protective wrapping with white Teflon tape is applied, which helps reduce light losses (Gramuglia et al., 2021) and has been used with scintillation detectors like CsI(Tl) (Vincent et al., 2023), followed by black vinyl tape, and then aluminum foil wrapping, to shield light coming into the crystal (Nishimura et al., 2022).

Gamma-rays are incident on the CsI(Tl) scintillator and are then detected as voltage signals by the MPPC before they are amplified and then reach the DP5 digital pulse processor. The MPPC array used has 64 (8 × 8) output channels but because we only required one output signal

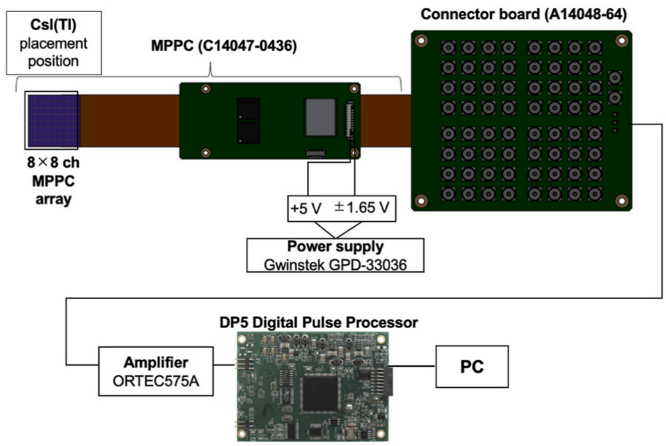

Fig. 1. Schematic overview of the complete prototype monitor setup. MPPC (C14047-0436, Hamamatsu photonics, Hamamatsu, Japan), and DP5 (Amptek Inc, Bedford, MA, USA).

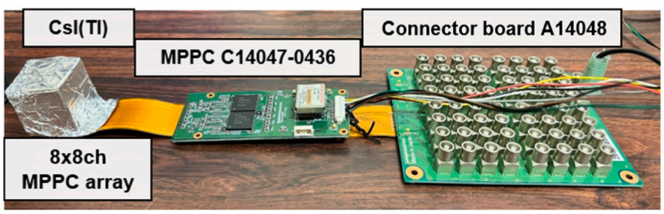

Fig. 2. Photograph of the main components of the prototype monitor CsI(Tl) scintillator (2.6 cm^3 cube), MPPC (C14047-0436, Hamamatsu photonics, Hamamatsu, Japan) and DP5 (Amptek Inc, Bedford, MA, USA).

from the scintillator, we extract the summed signal using the connector board seen in Fig. 2. Unlike a traditionally used multi-channel analyzer (MCA), the DP5 has the capabilities to internally store information about the pulse height and time-stamp data and send it to the connected PC (AMPTEK). Unlike a typical multi-channel analyzer, such as the MCA8000D, which can only store pulse height data, the DP5 stores both pulse height and time data for each detected event and sends it in real-time to the connected PC.

Apart from the prototype monitor, whose experimental setup is shown in Fig. 3, in this research, we utilize a High Purity Germanium (HPGe) detector (IGC 40190, Princeton Gamma-Tech Inc) and an NaI scintillation gamma-ray survey meter (Hitachi ALOKA TCS-171, Tokyo, Japan), both of which are verified detectors for such measurements (Knoll, 2010). The prototype monitor setup was encased in lead shielding, complemented by an additional layer of black cloth for enhanced shielding from light.

EMF Japan Co., Ltd is currently developing the actual device, which is being designed for wearability (such as around the neck), aiming for a weight comparable to that of a smartphone (~250 g). It will also feature a LED display to showcase the energy spectrum and dose rate data.

For the irradiation experiment, to produce gamma-rays with higher

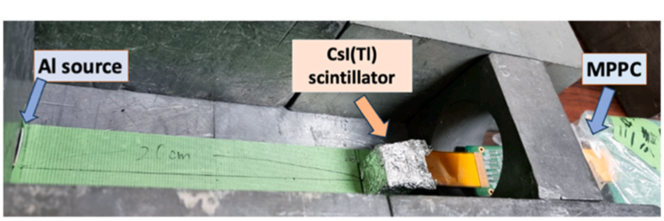

Fig. 3. Setup for measurement with the prototype monitor. Sources were placed 20 cm from the surface of the CsI(Tl) scintillator.

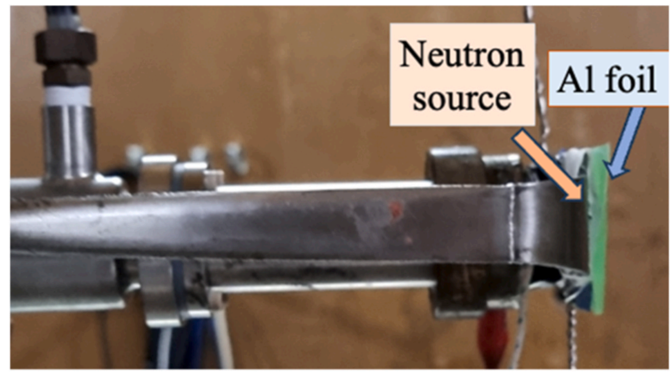

Fig. 4. Placement of the Al foil in front of the D-T neutron source at OKTAVIAN facility.

energy levels, a piece of aluminum plate measuring $2 \times 2 \times 0.1$ cm^3 was used. The plate was exposed to irradiation at the OKTAVIAN facility (Tamaki et al., 2022), a deuterium-tritium (D-T) neutron generator located at the University of Osaka, in Osaka, Japan, as depicted in Fig. 4. This facility's neutron source has the capability to emit 3×10^{12} fusion neutrons per second (Tamaki et al., 2022).

2.2. Methods

2.2.1. Sequential bayesian estimation

The pulse height spectrum is transformed into an energy spectrum using a process known as unfolding, or spectral deconvolution. This technique extracts the true information of the original incident radiation by solving the inverse problem (Sarzi Amadè et al., 2020; Bouchet, 1995) described by Eq. (1):

$$y_i = \sum_{j=1}^{n} R_{ij}\varphi_j \tag{1}$$

y_i: pulse height spectrum of gamma-rays.
R_{ij}: response function of the detector.
φ_j: energy spectrum of incident gamma-rays.

Solving of the unfolding problem can be achieved with various methods and algorithms. This study is based on the sequential Bayesian estimation, also known as the α-method. This approach in radiation measurement states that the energy spectrum can be deduced iteratively, as the gamma ray pulse-height data are received for each count by the detector. This methodology's effectiveness in radiation measurement has been validated by the foundational work of Iwasaki (Iwasaki, 1996) and Nauchi (Nauchi and Iwasaki, 2014).

Building on this foundation, our research group has developed an improved sequential Bayesian estimation method, termed the *k*-α method which expedites the convergence process of determining the energy spectrum and dose rate. As the developmental detail of this method has been described in detail by Kobayashi (Kobayashi et al., 2017), Nishimura (Nishimura et al., 2022), Voulgaris (Voulgaris et al., 2023), (Voulgaris et al., 2024) and Murata (Murata et al., 2024), we briefly summarize the key points of the method and how exactly the energy spectrum and dose rate are derived in real-time.

When one radiation is counted by a detector at pulse height channel *i*, the posterior probability of the energy spectrum at channel *j*, $P_{(j|i)}$, can be derived by the response function R_{ij}, according to Eq. (2):

$$P_{(j|i)} = \frac{R_{ij}\varphi_j}{\sum_{j=1}^{n} R_{ij}\varphi_j} \tag{2}$$

$P(j|i)$: posterior probability of the energy spectrum at a channel j, when radiation is counted by the detector at pulse height channel i.

The response function of the monitor is obtained through the use of experimental and simulation data (Nishimura et al., 2022; Kobayashi et al., 2017). Simulations using Monte Carlo methods, like MCNP5 (Monte Carlo N-Particle transport code 5) (Goorley, 2013) are integrated with experimental data in order to account for the prototype's energy resolution. Such hybrid methods of experiment and simulation are known to produce accurate response functions (Wang et al., 2012). The intrinsic detection efficiency at each energy is inherently included in the response function generated by MCNP5, while the experimentally measured energy resolution is incorporated in the response function through Gaussian broadening of the simulated spectra.

The energy spectrum φ_j is derived from:

$$\varphi_j' = (1-\alpha)\varphi_j + \alpha \frac{R_{ij}\varphi_j}{\sum_{j=1}^{n} R_{ij}\varphi_j} \tag{3}$$

α: Index related to effect of prior to posterior probability.
φ_j': Energy spectrum revised by the latest detected count.
φ_j: Estimated energy spectrum before the last count.

Revision is conducted with each count, meaning each pulse height signal on the i channel.

By assigning the posterior probability as prior probability for the new data, successive estimations are possible. The parameter α affects the contribution of the prior probability to the estimation. However, the convergence of this method is slow. We found that it can be accelerated with the addition of a parameter ***k*** that satisfies Eq. (4):

$$\alpha = \frac{1+kN}{N} \left(\alpha = 1, \text{if } \mathrm{N} < \frac{1}{1-\mathrm{k}}\right) \tag{4}$$

k: parameter to accelerate convergence, which is dependent on count rate.
N: count number.

Parameter *k* plays a crucial role in the convergence of the estimation process. It determines the rate at which the energy spectrum is revised with each count. A larger k value leads to faster convergence, but it may also result in instability. On the other hand, a smaller k value leads to slower convergence but provides more stable results. The optimum k value depends on the measurement conditions such as the count rate, and the desired balance between convergence speed and accuracy of measurement.

With this *k-a* method, the energy spectrum is estimated in real-time, for each count, during measurement. The dose rate is then calculated by applying a dose conversion coefficient to the estimated energy spectrum.

2.2.2. Dose rate estimation

As mentioned in section 2.1, by replacing a traditionally used MCA in the setup with a DP5 digital pulse processor, true real-time estimation is made possible. The obtained signal, which contains information on pulse height and time-list data, is fed into custom programs that we have developed. This includes a program for executing the k-α method and two additional programs: one for the real-time visualization of the energy spectrum and dose rate, and another for saving this data in.csv files (Voulgaris et al., 2023).

From the estimated gamma-ray energy spectrum described above, the dose rate is then calculated in real-time according to Eq. (5).

$$D = \sum_{j=1}^{n} d_j \cdot \frac{C_j}{ST} \tag{5}$$

D: Dose rate (μSv/h).
j: Indicates the energy bin.
d_j: Effective dose rate per unit fluence $(\mu\mathrm{Sv/h})/(\mathrm{cm}^{-2}\cdot\mathrm{s}^{-1})$ (flux-to-dose conversion coefficient)(ICRP, 1997)
C_j: Number of counts.
S: Area of the surface of the scintillation detector (cm^2)
T: Time of measurement (s)

For ϕ_j being the flux per unit area and time in energy bin j $(/\mathrm{cm}^2/\mathrm{s})$ of the gamma-ray energy spectrum, Eq. (5) can be rewritten as:

$$D = \sum_{j=1}^{n} d_j \cdot \phi_j \tag{6}$$

2.2.3. Neutron irradiation

To produce high energy gamma-rays, an aluminum plate (measuring $2 \times 2 \times 0.1$ cm^3) was irradiated with D-T neutrons in order to induce the $^{27}Al(n,\alpha)^{24}Na$ reaction. This reaction produces the radioactive isotope ^{24}Na, which decays by beta-particle emission into the second excited state of ^{24}Mg. Subsequent transitions to the first excited state and finally to the ground state result in emission of gamma-rays with energies of 2.755 MeV and 1.369 MeV, respectively (Nakao et al., 2021; Bé, 2004). The half-life of ^{24}Na is recorded as 14.9581 h (Chechev and Kuzmenko, 2016).

The ^{24}Na method was selected for its reproducibility and because it does not generate any form of radioactive waste (Epp and Griffin, 2003).

To estimate the theoretical dose rate at a specified distance, Eq. (6) was employed (Canadian Nuclear Safety Commission, 2017; IAEA, 1986):

$$D = \Gamma \times \frac{Q}{r^2} \tag{6}$$

Γ: effective dose rate constant ($\mu\mathrm{Sv}\cdot\mathrm{m}^2\cdot\mathrm{MBq}^{-1}\cdot\mathrm{h}^{-1}$)
Q: radioactivity (MBq)
r: detector-source distance (m)

Knowing the detection efficiency of a detector allows for calculation of the absolute activity of a source. Thus, to calculate the radioactivity of the ^{24}Na, calculating the detection efficiency was necessary (Knoll, 2010). Neutron irradiation experiments were conducted using the D-T neutron source (Tamaki et al., 2022), with irradiation time of 8.5 h. After irradiation, the aluminum plate was retrieved, and measurements with the following devices were performed.

- Prototype real-time monitor: Measurements were conducted at a distance of 20 cm, with both the energy spectrum and dose rate were recorded in video format, as well as saved in the form of.csv files.
- High Purity Germanium (HPGe) Radiation Detector. The source was placed 10 cm from the detector receiving surface, and both were shielded completely with lead. The detector was calibrated using standard sources of ^{137}Cs, ^{60}Co and ^{22}Na. Having known activities and half-lives, the amount of gamma-rays produced was calculated. By calculating the detection efficiency of the detector for each energy and applying the least squares method, fitting of the 1.369 MeV peak of ^{24}Na was applied. Knowing the detection efficiency, time since irradiation, measurement time, net areas of the ^{24}Na peaks and emission ratio, the radioactivity Q of Eq. (6) at the time measured by the prototype monitor by means of Eq. (7) was calculated:

$$Q = A_0 \cdot e^{-\lambda(t_2 - t_1)} \tag{7}$$

A_0: activity at start of measurement with the HPGe detector.
t_2: Prototype monitor measurement start time (s)
t_1: HPGe detector measurement start time (s)

λ: radioactive decay constant = ln(2)/(half-life)

- NaI(Tl) survey meter (Hitachi ALOKA, Tokyo, Japan). Multiple dose rate readings were recorded at the same distance of 20 cm.

3. Results and discussion

3.1. Results

The gamma-rays were measured by the prototype monitor and the energy peaks were accurately detected and observed in real-time.

Fig. 5 shows the pulse height spectra obtained from the HPGe detector measurement.

Fig. 6 displays on the top part the true information of the measured gamma-rays, the unfolded energy spectrum. Comparing with Fig. 5, two discrete gamma-rays from ^{24}Na are clearly observed in Fig. 6. Other discrepancies will be discussed in Section 3.2. On the bottom of Fig. 6 the real-time graph of the estimated dose rate is shown (see also Fig. 7, which presents a screenshot of the prototype monitor interface during real-time measurement).

The theoretical dose rate has been calculated (4.05 ± 0.22 μSv/h), using the methods described in section 2.2.3. It is presented alongside the experimental results from real-time measurements (4.07 μSv/h and standard deviation 0.37% (±0.02)) and NaI survey meter (3.83 μSv/h) in Fig. 8. The statistical error of the survey meter is 3.40%. The deviations of the measurements from the theoretical value are 0.40% and 5.43% for the prototype monitor and the survey meter respectively. These results illustrate the consistency between the prototype monitor and the theoretical calculations, considering the uncertainties in activity measurement, efficiency calibration, detector positioning, decay corrections, self-attenuation of gamma rays in the aluminum foil, dose rate constant, and statistical variations in detector count rates.

Regarding the convergence time of the dose-rate, by setting the parameter *k* according to the count rate of the present experiment, the dose-rate value stabilizes after about 18-20 s, as shown in Fig. 9.

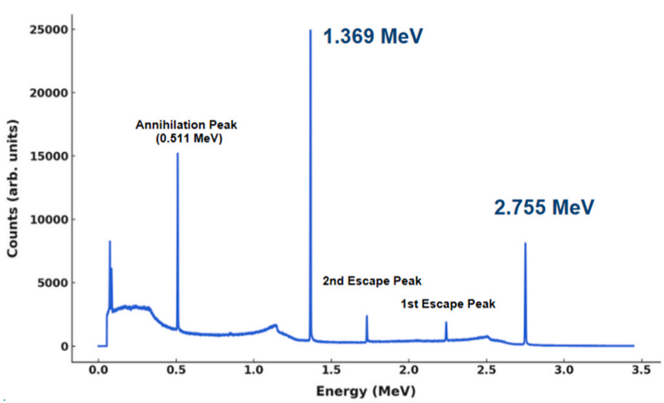

Fig. 5. Pulse height spectra of ^{24}Na, obtained with the HPGe detector.

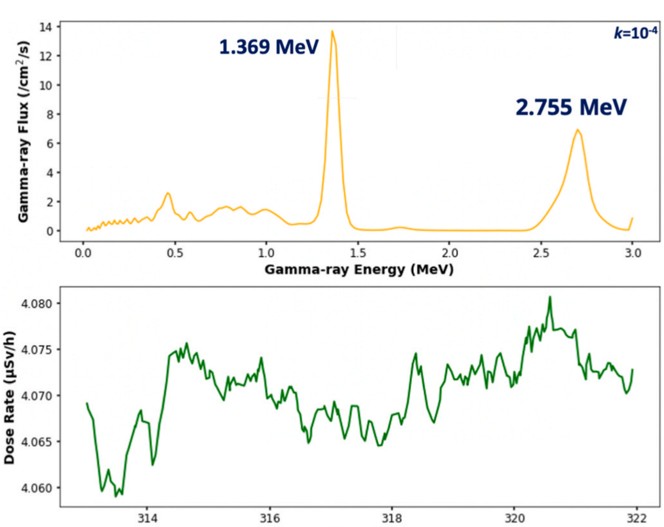

Fig. 6. Unfolded energy spectra of ^{24}Na (top); dose rate (bottom) obtained with the prototype monitor.

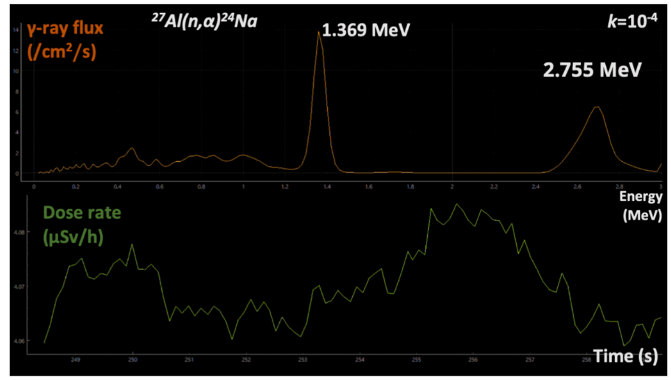

Fig. 7. Annotated screenshot of real-time measurement. Gamma-ray flux (top) and dose rate (bottom) are visualized in real-time (in seconds). The 1.369 and 2.755 MeV gamma-rays from ^{24}Na are clearly visible.

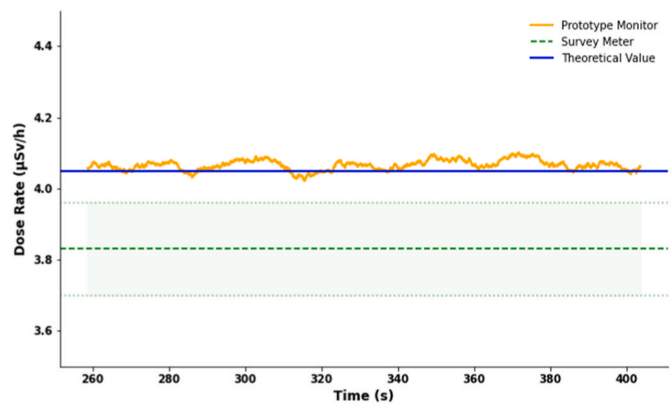

Fig. 8. Comparison of measured dose rates: Prototype monitor, NaI survey meter, and theoretical value. The statistical error of the survey meter is 3.40%.

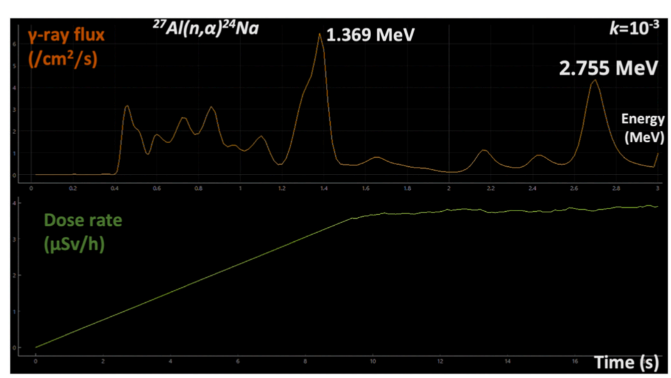

Fig. 9. Annotated screenshot of the prototype's interface at the start of measurement during real-time unfolding. Gamma-ray flux and dose rate are visualized in real-time. Dose rate is updated rapidly early on to approach the correct value and gradually stabilizes with slight fluctuations.

3.2. Discussion

The prototype monitor's ability to measure the energy spectrum and the dose rate of gamma-rays up to 3 MeV addresses a critical need in radiation safety for medical workers, given the limitations of traditional dosimetry devices, which may fail to provide real-time data or accurate dose estimations across a broad spectrum of gamma-ray energies.

Regarding the energy spectrum estimation, as seen in the top graph of Fig. 6, the unfolded spectrum was successfully visualized in real-time. Unwanted noise and peaks, such as the escape peaks visible in the pulse height distribution of the HPGe detector measurement, were removed and the true information of the incoming gamma-rays was restored.

The pulse height distribution is the raw output of a detector, which often contains distortions due to the geometry and materials. Therefore, radiation spectrum unfolding is necessary to reconstruct the undisturbed, original energy spectrum. For instance, the 0.511 MeV annihilation peak is absent in the unfolded spectrum because it is already incorporated in the response function of the prototype monitor. During the creation of the response function, sources exceeding 1.022 MeV were utilized, which resulted in the production of annihilation gamma-rays outside the detector, contributing to this peak. In contrast, the 0.511 MeV peak is visible in the pulse height distribution presented in Fig. 5, as it shows the unprocessed raw data from the HPGe detector without unfolding. Through the unfolding process, distortions such as the annihilation peak are corrected, accurately restoring the original source spectrum. Although a small residual peak remains near 0.5 MeV in the unfolded spectrum, seen in Fig. 6, this is attributed to minor artifacts introduced during the unfolding process.

The dose rate measurements and calculations conducted, support the potential of the prototype monitor. The prototype's measured dose rate closely matched with the theoretical value, while the NaI survey meter showed expected differences when compared to them, due to its calibration using a ^{137}Cs source at 0.662 MeV. As demonstrated in Fig. 8, the NaI survey meter underestimated the dose rate for higher energy gamma-rays. The survey meter used in this study has an error tolerance of ±15% for digital readings. The measured value was 3.83 μSv/h, which is within the maximum expected error window specified for the instrument. The theoretically derived value was 4.05 μSv/h, with an uncertainty of ±0.22 μSv/h considering the effects of activity related components such as HPGe detector efficiency calibration, decay corrections, self-attenuation, and detector positioning. Devices calibrated at a single energy point tend to overestimate dose rates at energies below the calibration point and underestimate at energies above it (Nishimura et al., 2022). The prototype monitor is not subject to these calibration constraints due to its capacity for direct, real-time energy spectrum measurement and application of flux-to-dose conversion coefficient, allowing for accurate dose estimation across a broad range of gamma-ray energies. This addresses the discrepancy observed in Fig. 8, as the prototype monitor's dose rate aligns closely with the theoretical dose rate, while the survey meter exhibits an underestimation due to its inherent calibration related limitations.

By setting the parameter k of the k-α method accordingly, convergence to a stable value is achieved in around 18-20 s as shown in Fig. 9. With the k-α method early on the convergence is very fast (parameter α of Equation (4) is large) and later on the convergence slows down in order to increase accuracy (α becomes smaller). This rapid initial monotonical increase shows how fast the dose rate approaches the correct dose rate value and then when it is close to the correct value the fluctuations are observed. Implementing an adaptive algorithm that adjusts dynamically the parameter k based on the real-time count rate is also being considered. This will allow for the monitor to be able to account for count rate fluctuations in medical radiation environments and enhance its performance capabilities. For comparison, when setting the time constant to 30 s in the NaI survey meter, it requires approximately 90 s to produce a stable result. Same time constant value of the NaI survey meter has been selected in other research (Sanami et al., 2021) and was chosen in order to increase its accuracy. The results highlight the prototype monitor's advantage in environments with gamma-rays close to 3 MeV.

The ability of the monitor to simultaneously display the unfolded energy spectrum and dose rate in real time, can contribute meaningfully to practical applications. Conventional spectrometers typically display only the pulse height spectrum. In contrast, the prototype monitor displays the unfolded gamma-ray spectrum in real time, enabling clearer identification of radionuclides and in general a more accurate understanding of what the radiation environment actually looks like. In combination with the real-time dose rate display, we believe it helps in both operational decision-making, understanding of exposure risks, and source characterization.

4. Conclusion

The results showed that our prototype real-time gamma-ray monitor can accurately display the energy spectrum and dose rate simultaneously and in real-time for gamma-rays with energies of up to 2.755 MeV. We hope that this device will contribute to the progress of real-time gamma-ray monitoring, especially in medical environments utilizing radiation, where energies can be up to 3 MeV. The experimental results agree with the theoretical results, establishing the prototype's effectiveness in such environments. It should be noted that this level of agreement was achieved under the fixed geometry of the experimental setup in OKTAVIAN, therefore in clinical settings, geometric and other scattering conditions are expected to be sources of additional uncertainty. The prototype monitor is straightforward to use and meets a crucial need in radiation safety, providing in real-time information that is useful in informing medical workers about their exposure. It contributes to the field of gamma-ray exposure monitoring solutions thanks to its advantages in dose rate accuracy and portability similar to a dosimeter, along with providing detailed information like a spectrometer, with the benefit of displaying the unfolded, true gamma-ray energy spectrum, not just the pulse height distribution.

Currently, we are aiming to extend the prototype's range of detection to include even higher energy gamma-rays of up to 10 MeV, along with research in separating gamma-ray and neutron contributions, thus increasing the potential applications of the prototype monitor.

CRediT authorship contribution statement

Nikolaos Voulgaris: Writing – review & editing, Writing – original draft, Visualization, Validation, Software, Resources, Project administration, Methodology, Investigation, Formal analysis, Data curation, Conceptualization. **Jiye Qiu:** Writing – review & editing, Software, Investigation, Data curation. **Shingo Tamaki:** Writing – review & editing, Supervision, Software, Methodology, Formal analysis, Data curation, Conceptualization. **Sachie Kusaka:** Writing – review & editing, Visualization, Project administration, Methodology. **Isao Murata:** Writing – review & editing, Supervision, Resources, Project administration, Methodology, Investigation, Conceptualization.

Funding sources

This research did not receive any specific grant from funding agencies in the public, commercial, or not-for-profit sectors.

Declaration of competing interest

The authors declare that they have no known competing financial interests or personal relationships that could have appeared to influence the work reported in this paper.

Data availability

Data will be made available on request.

References

Alsaab, A.H., Zeghib, S., 2023. Analysis of X-ray and gamma ray shielding performance of prepared polymer micro-composites. J. Radiat. Res. Appl. Sci. 16 (4), 100708. https://doi.org/10.1016/j.jrras.2023.100708.

AMPTEK. DP5 OEM digital pulse processor & MCA – amptek – x-ray detectors and electronics. In: https://www.amptek.com/products/digital-pulse-processors/dp5-digital-pulse-processor-and-mca.

Bakshi, J., Chu, B.P., 2020. Attenuation of gamma radiation using clear view radiation shielding TM in nuclear power plants. Hospitals and Radiopharmacies Health Phys. 119 (6), 776. https://doi.org/10.1097/HP.0000000000001336.

Bureau international des poids et mesures. In: Bé, M.-M. (Ed.), 2004. Table of Radionuclides, 1. A=1 to 150 (BIPM, Sèvres). https://www.bipm.org/en/publications/monographies.

Bouchet, L., 1995. A comparative study of deconvolution methods for gamma-ray spectra. Astron. Astrophys., Suppl. Ser. 113, 167. https://ui.adsabs.harvard.edu/abs/1995A%26AS..113..167B%2F/abstract.

Buzhan, P., Karakash, A., Teverovskiy, Yu, 2018. Silicon Photomultiplier and CsI(Tl) scintillator in application to portable H*(10) dosimeter. Nucl. Instrum. Methods Phys. Res. Sect.Accel. Spectrometers Detect. Assoc. Equip. 912, 245. https://doi.org/10.1016/j.nima.2017.11.067.

Canadian Nuclear Safety Commission, 2017. Radionuclide information booklet (Canadian Nuclear Safety Commission). https://publications.gc.ca/site/eng/9.822446/publication.html.

Chechev, V.P., Kuzmenko, N.K., 2016. Decay Data Evaluation Project (DDEP): updated decay data evaluations for ^{24}Na, ^{46}Sc, ^{51}Cr, ^{54}Mn, ^{57}Co, ^{59}Fe, ^{88}Y, ^{198}Au. Appl. Radiat. Isot. 109, 139. https://doi.org/10.1016/j.apradiso.2015.11.009.

Długosz-Lisiecka, M., Biegała, M., Jakubowska, T., 2023. Activation of medical accelerator components and radioactive waste classification based on low beam energy model Clinac 2300. Radiat. Phys. Chem. 205, 110730. https://doi.org/10.1016/j.radphyschem.2022.110730.

Donadille, L., Trompier, F., Robbes, I., Derreumaux, S., Mantione, J., Asselineau, B., Amgarou, K., Martin, A., Bottollier-Depois, J.F., Queinnec, F., Aubert, B., Clairand, I., 2008. Radiation protection of workers associated with secondary neutrons produced by medical linear accelerators. Radiat. Meas. 43 (2–6), 939. https://doi.org/10.1016/j.radmeas.2008.01.018.

Epp, E.M., Griffin, H.C., 2003. Use of ^{24}Na as a γ-ray calibration source above 3 MeV. Nucl. Instrum. Methods Phys. Res. Sect. Accel. Spectrometers Detect. Assoc. Equip. 505 (1–2), 9. https://doi.org/10.1016/S0168-9002(03)01008-8.

Ghassemi, A., Sato, K., Kobayashi, K., 2022. MPPC technical guide to silicon photomultipliers (MPPC), Hamamatsu Photonics K.K., Doc. No. KAPD9005E. https://www.hamamatsu.com/content/dam/hamamatsu-photonics/sites/documents/99_SALES_LIBRARY/ssd/mppc_kapd9005e.pdf.

Goorley, J., 2013. MCNP5 to MCNP6 migration notes LA-UR-13-23338. 1079560. https://www.osti.gov/servlets/purl/1079560/.

Gramuglia, F., Frasca, S., Ripiccini, E., Venialgo, E., Gâté, V., Kadiri, H., Descharmes, N., Turover, D., Charbon, E., Bruschini, C., 2021. Light extraction enhancement techniques for inorganic scintillators. Crystals 11 (4), 362. https://doi.org/10.3390/cryst11040362.

IAEA, 1986. In: Decay Data of the Transactinium Nuclides. IAEA, Vienna. https://nds.iaea.org/records/qz79k-4v692.

IAEA, 2018. Radiation Protection and Safety in Medical Uses of Ionizing Radiation: Specific Safety Guide. IAEA, Vienna. https://www-pub.iaea.org/MTCD/Publications/PDF/PUB1775_web.pdf.

ICRP, 1997. Conversion Coefficients for Use in Radiological Protection Against External Radiation. Pergamon Press, Oxford, p. 1.

Iwasaki, S., 1996. A new approach for unfolding PHA problems based only on the Bayes theorem. In: Hamid, A., Bohumil, O. (Eds.), Proceedings of the 9th International Symposium on Reactor Dosimetry. American Society for Testing and Materials Euratom Working Group on Reactor Dosimetry & E.N. Society. World Scientific, Prague, Czech Republic, p. 245.

Jasni, A.A., Yap, Y., Hashim, I.H., Ahmad, N.E., Ramlee, N., 2021. Two dimensional array of MPPC and CsI(Tl) for radiation monitoring prototype. IOP Conf. Ser. Mater. Sci. Eng. 1106 (1), 012028. https://doi.org/10.1088/1757-899X/1106/1/012028.

Kataoka, J., Kishimoto, A., Fujita, T., Nishiyama, T., Kurei, Y., Tsujikawa, T., Oshima, T., Taya, T., Iwamoto, Y., Ogata, H., Okochi, H., Ohsuka, S., Ikeda, H., Yamamoto, S., 2015. Recent progress of MPPC-based scintillation detectors in high precision X-ray and gamma-ray imaging. Nucl. Instrum. Methods Phys. Res. Sect. Accel. Spectrometers Detect. Assoc.Equip. 784, 248. https://doi.org/10.1016/j.nima.2014.11.004.

Kato, T., Kataoka, J., Nakamori, T., Miura, T., Matsuda, H., Kishimoto, A., Sato, K., Ishikawa, Y., Yamamura, K., Nakamura, S., Kawabata, N., Ikeda, H., Yamamoto, S., Kamada, K., 2013. A novel gamma-ray detector with submillimeter resolutions using a monolithic MPPC array with pixelized Ce:LYSO and Ce:GGAG crystals. Nucl. Instrum. Methods Phys. Res. Sect. Accel. Spectrometers Detect. Assoc. Equip. 699, 235. https://doi.org/10.1016/j.nima.2012.04.008.

Knoll, G.F., 2010. In: Radiation Detection and Measurement, fourth ed. John Wiley, Hoboken, N.J.

Kobayashi, M., Sato, F., Kusaka, S., Murata, I., 2017. Feasibility study on real-time γ-ray spectrum/dose measurement system. EPJ Web Conf. 153, 07014. https://doi.org/10.1051/epjconf/201715307014.

Lakhwani, O.P., Dalal, V., Jindal, M., Nagala, A., 2019. Radiation protection and standardization. J. Clin. Orthop. Trauma 10 (4), 738. https://doi.org/10.1016/j.jcot.2018.08.010.

Lee, W.J., Jang, E.J., Kim, K.S., Bang, Y.J., 2022. Underestimation of radiation doses by compliance of wearing dosimeters among fluoroscopically-guided interventional medical workers in Korea. Int. J. Environ. Res. Publ. Health 19 (14), 8393. https://doi.org/10.3390/ijerph19148393.

Matsumura, H., Yoshida, G., Toyoda, A., Masumoto, K., Nakamura, H., Miura, T., Nishikawa, K., Bessho, K., Akita, T., Katsuta, S., Akimoto, T., Sugama, Y., Nobuhara, F., Nagashima, Y., 2022. Investigation of concrete radioactivation in cyclotron type proton therapy facilities using in situ 24Na measurement method. Radiat. Saf. Manag. 21, 13. https://doi.org/10.12950/rsm.200909 [0].

Meier, J., Kappadath, S.C., 2015. Characterization of the energy response and backscatter contribution for two electronic personal dosimeter models. J. Appl. Clin. Med. Phys. 16 (6), 423. https://doi.org/10.1120/jacmp.v16i6.5549.

Ministry of the Environment, 2019. Booklet to Provide Basic Information Regarding Health Effects of Radiation (Radiation Health Management Division,Environmental Health Department. Minister's Secretariat, Ministry of the Environment, Government of Japan). https://www.env.go.jp/en/chemi/rhm/basic-info/.

Moiseev, D.V., Lukina, L.I., 2020. Improving the accuracy of gamma radiation measurements in radiation monitoring. In: IOP Conf. Ser. Earth Environ. Sci., 548, 032009. https://doi.org/10.1088/1755-1315/548/3/032009, 3.

Murata, I., Voulgaris, N., Miyoshi, T., Shinohara, M., Nishimura, H., Kobayashi, M., Kusaka, S., Tamaki, S., Sato, F., 2024. Real-time gamma-ray energy spectrum/dose monitor with k-α method based on sequential bayesian estimation. Appl. Radiat. Isot. 212, 111454. https://doi.org/10.1016/j.apradiso.2024.111454.

Nakao, N., Kajimoto, T., Sanami, T., Froeschl, R., Iliopoulou, E., Infantino, A., Yashima, H., Oyama, T., Nagaguro, S., Lee, E., Matsumoto, T., Masuda, A., Uwamino, Y., Roesler, S., Brugger, M., 2021. Measurements and Monte Carlo simulations of high-energy neutron streaming through the access maze using activation detectors at 24 GeV/c proton beam facility of CERN/CHARM. J. Nucl. Sci. Technol. 58 (8), 899. https://doi.org/10.1080/00223131.2021.1887003.

Nauchi, Y., Iwasaki, S., 2014. Convergence of unfolded spectrum with response function for single radiation based on Bayes' theorem. Nucl. Instrum. Methods Phys. Res. Sect. Accel. Spectrometers Detect. Assoc. Equip. 735, 437. https://doi.org/10.1016/j.nima.2013.09.064.

Nishimura, H., Shinohara, M., Miyoshi, T., Voulgaris, N., Kusaka, S., Tamaki, S., Sato, F., Murata, I., 2022. Experimental verification of real-time gamma-ray energy spectrum and dose monitor. Appl. Radiat. Isot. 185, 110226. https://doi.org/10.1016/j.apradiso.2022.110226.

Nuclear Regulation Authority, 2017. Method for measurement of environmental gamma-rays with a continuous monitor (No.17). In: The Series of Environmental Radioactivity Measuring Methods. https://www.envraddb.go.jp/en/special/measuring-methods/.

Okazaki, K., Tanaka, H., Takata, T., Kawabata, S., Hu, N., Matsubayashi, N., Mukawa, T., Sakurai, Y., Suzuki, M., 2023. Development of a prompt gamma-ray detector with an 8 × 8 array LaBr 3(Ce) scintillator and a multi-pixel photon counter for boron neutron capture therapy. Nucl. Instrum. Methods Phys. Res. Sect. Accel. Spectrometers Detect. Assoc. Equip. 1055, 168546. https://doi.org/10.1016/j.nima.2023.168546.

Ortega, X., Ginjaume, M., 2000. Advantages and limitations of electronic devices for primary occupational dosimetry. In: International ISOE Symposia. ISOE, Tarragona, Spain. In: https://www.isoe-network.net/publications/pub-proceedings/symposia/international-symposia/tarragona-spain-april-2000/papers-18/171-ortega2000.html.

Otto, T., 2016. Personal dose-equivalent conversion coefficients for 1252 radionuclides. Radiat. Protect. Dosim. 168 (1), 1. https://doi.org/10.1093/rpd/ncu316.

Pereira, M. da C.C., Madi Filho, T., Lopes, V.M., Berretta, J.R., Cardenas, J.P.N., 2015. Scintillation response of CsI: tl crystal under neutron, gamma, alpha particles and beta excitations. international nuclear Atlantic conference. Brazilian nuclear program. State policy for a sustainable world; 12. In: ENAN: Meeting on Nuclear Applications (INAC 2015), Sao Paulo, SP (Brazil). https://inis.iaea.org/records/kg76j-k1h23.

Piotrowski, I., Dawid, A., Kulcenty, K., Suchorska, W.M., 2021. Use of biological dosimetry for monitoring medical workers occupationally exposed to ionizing radiation. Radiation 1 (2), 95. https://doi.org/10.3390/radiation1020009.

Polaczek-Grelik, K., Kawa-Iwanicka, A., Rygielski, M., Michalecki, Ł., 2019. In: Almayah, B.A. (Ed.), Use of Gamma Radiation Techniques in Peaceful Applications. IntechOpen. https://doi.org/10.5772/intechopen.78481.

Qureshi, F., Ramprasad, A., Derylo, B., 2022. Radiation monitoring using personal dosimeter devices in terms of long-term compliance and creating a culture of safety. Cureus 14 (8), e27999. https://doi.org/10.7759/cureus.27999.

Risse, M., Friedrich, H., Glabian, J., Köble, T., Schumann, O., Teuteberg, T., 2023. Comparison of CLYC vs. CsI in a hand-held detector. EPJ Web Conf. 288, 10009. https://doi.org/10.1051/epjconf/202328810009.

Sanami, T., Sasaki, S., Iijima, K., Kishimoto, Y., Saito, K., 2021. Time Variations in Dose Rate and γ Spectrum Measured at Tsukuba City, Ibaraki, due to the Accident of Fukushima Daiichi Nuclear Power Station. Insights Concerning the Fukushima Daiichi Nuclear Accident, 4. The Atomic Energy Society of Japan, p. 11. https://www.aesj.net/publish/fukushima_insights_intro/volume-4.

Sarzi Amadè, N., Bettelli, M., Zambelli, N., Zanettini, S., Benassi, G., Zappettini, A., 2020. Gamma-Ray spectral unfolding of CdZnTe-Based detectors using a genetic algorithm. Sensors 20 (24), 7316. https://doi.org/10.3390/s20247316.

Sasaki, M., Fujibuchi, T., 2020. Development of the system of radiological protection and medical exposure: basic information and trends. Radiat. Environ. Med. 9 (2), 105. https://remcp.hirosaki-u.ac.jp/rem_archive/radiation-environment-and-medicine-vol-9-no-2/.

Sharma, S., Sarkar, M.S., 2020. Measurement and simulation of gamma-ray background in a low energy accelerator facility. J. Instrum. 15 (9), T09003. https://doi.org/10.1088/1748-0221/15/09/T09003.

Tamaki, S., Panuntun, F., Uedoi, K., Haidong, W., Kusaka, S., Manabe, Y., Akiyama, Y., Tanaka, T., Sato, F., Murata, I., 2022. Radioactivation analysis of concrete wall in OKTAVIAN facility. Plasma Fusion Res. 17 (0), 1405001. https://doi.org/10.1585/pfr.17.1405001.

Torigoe, K., Fukazawa, Y., Galgóczi, G., Mizuno, T., Nakazawa, K., Ohno, M., Pál, A., Takahashi, H., Tanaka, K., Tarcai, N., Uchida, N., Werner, N., Enoto, T., Frei, Z., Ichinohe, Y., Kiss, L., Odaka, H., Řípa, J., Várhegyi, Z., 2019. Performance study of a large CsI(Tl) scintillator with an MPPC readout for nanosatellites used to localize gamma-ray bursts. Nucl. Instrum. Methods Phys. Res. Sect. Accel. Spectrometers Detect. Assoc. Equip. 924, 316. https://doi.org/10.1016/j.nima.2018.08.039.

Vincent, K.N., Mahapatra, S., Poddar, I., Verma, S., 2023. Improving the resolution and light yield in CsI(Tl) scintillators. Nucl. Instrum. Methods Phys. Res. Sect. Accel. Spectrometers Detect. Assoc. Equip. 1056, 168624. https://doi.org/10.1016/j.nima.2023.168624.

Voulgaris, N., Miyoshi, T., Tamaki, S., Kusaka, S., Murata, I., 2023. Development of real-time gamma-ray spectrum and dose monitor: investigation of true real-time convergence. In: Proceedings of the 37th Workshop on Radiation Detectors and Their Uses (High Energy Accelerator Research Organization (KEK). Tsukuba, Ibaraki, Japan. https://lib-extopc.kek.jp/preprints/PDF/2023/2325/2325001.pdf.

Voulgaris, N., Nishimura, H., Tamaki, S., Kusaka, S., Murata, I., 2024. Balancing performance and portability: a study on CsI(Tl) crystal sizes for real-time gamma-ray spectrum and dose monitoring. Radiation 4 (3), 213. https://doi.org/10.3390/radiation4030016.

Wang, J., Wang, Z., Peeples, J., Yu, H., Gardner, R.P., 2012. Development of a simple detector response function generation program: the CEARDRFs code. Appl. Radiat. Isot. 70 (7), 1166. https://doi.org/10.1016/j.apradiso.2011.11.003.

Yamamoto, T., Yanagida-Miyamoto, Y., Iida, T., Nanto, H., 2020. Current status and future prospect of RPL glass dosimeter. Radiat. Meas. 136, 106363. https://doi.org/10.1016/j.radmeas.2020.106363.

Yanagida, T., 2018. Inorganic scintillating materials and scintillation detectors. Proc. Jpn. Acad. Ser. B 94 (2), 75. https://doi.org/10.2183/pjab.94.007.

Yanagida, T., Okada, G., Kato, T., Nakauchi, D., Kawaguchi, N., 2022. A review and future of RPL dosimetry. Radiat. Meas. 158, 106847. https://doi.org/10.1016/j.radmeas.2022.106847.